

Performance enhancement of 5G uplink MIMO over fading-shadowing, path losses, and ISI using LZF equalizer

Ashwaq Q. Hameed¹, Ali H. Numan²

¹Department of Electrical Engineering, University of Technology, Baghdad, Iraq

²Department of Electromechanical Engineering, University of Technology, Baghdad, Iraq

Article Info

Article history:

Received Oct 28, 2022

Revised Dec 21, 2022

Accepted Feb 23, 2023

Keywords:

5G multi-input multi-output

Inter symbol interference

Linear zero-forcing equalizer

Path losses

Shadowing

Uplink system

ABSTRACT

The challenges of the 5G mobile wireless communication systems transmission channels have been changed continuously because of the signal transfer path characteristics such as real-time applications, path loss, multiple users, reflected rays, channel Rayleigh-fading, shadowing, noise, and inter symbol interference (ISI). These challenges have been treated to reach the minimum bit error rate (BER) value of the received data and maximum data rate of high-speed wireless mobile communication systems. In this paper, the linear zero-forcing (LZF) equalizer with uplink multi-input multi-output (MIMO) system has been proposed to enhancement the BER, which is caused by the ISI, Rayleigh fading, shadowing, path losses, and additive white gaussian noise (AWGN). Furthermore, the proposed approach is applied to a different number of antennas constellation to show the effect of increasing the number of antennas on the BER. The results show that the proposed LZF equalizer-MIMO system model has reached lower BER values, and high performance with an increase in the receiver to 8×14 , 8×16 and 8×18 antennas constellation at 8, 10, 12, 14, 16, and 18 dB signal to noise ratio (SNR).

This is an open access article under the [CC BY-SA](#) license.



Corresponding Author:

Ashwaq Q. Hameed

Department of Electrical Engineering, University of Technology

Al-Senaa Street, Baghdad, Iraq

Email: ashwaq.q.hameed@uotechnology.edu.iq

1. INTRODUCTION

The performance of the next generation 5G wireless communication systems can be measured through transmission channels which depend on essential parameters such as the channel Rayleigh fading, multipath, inter symbol interference (ISI), multiple reflection rays, path loss, and the effects of shadowing, which cause performance delay. The improvement of the wireless communication environment has been increased due to the multi-carrier mobile channels, internet applications, intranet, and Bluetooth system that need huge constant arrival transmission, high data rate, reliability, quality of service (QoS), minimized bit error rate (BER), spectrum diversity, and efficiency gain [1], [2]. Furthermore, the shadowing effect on the spectral efficiency has been considered for the cell limit of users in inhomogeneous networks and is analyzed in [3].

The effect of shadowing on the spectral efficiency of macro-femto and macro-only networks has been compared. Then the shadowing effects of the macro-femto have been neglected compared to the macro-only network. The spectral efficiency can be reduced by shadowing and fading the macro network with increased mobile user interference. In contrast, the effect on the macro-femto network is negligible. The reliability analysis of wireless links for IoT applications under shadow conditions has been presented [4], [5]. The non-orthogonal multiple access outage performance with interference over κ - μ shadowed fading

channels was analyzed. Treating the wireless communication system challenges provides many merits, such as increasing the capacity and decreasing the interference caused by the co-channel [6]. The multipath-fading has been obtained by small-scale-fading, which presents random and fast signal strength variations at the receiving antennas.

Furthermore, the large scale-fading can produce shadowing effects due to large structures. Small and large scale-fading can be modelled based on lognormal distribution and Rayleigh, Nakagami, and Rice distribution respectively [7]. On the other hand, the energy and spectral efficiencies of m-ary continuous phase frequency shift keying (M-CPFSK) are tested for additive white gaussian noise (AWGN) with multipath shadowed fading channels [8].

Many models of relay selection protocols can be used for a mobile wireless network for shadowing and side multipath of information, like techniques for worse selection of best channel, nearest-neighbour selection, techniques for partial relay selection, and reactive-relay selection. These techniques can be operated in the range of millimeter-wave (60 GHz to higher) frequencies. Therefore, the transmission data can be increased cause the relay protocols can be faster over time [9], [10]. In addition, the two-dimensional models of the site-to-site cross-correlation of shadow, fading, and autocorrelation filters algorithm can be used with linear-interpolation techniques to provide low computational complexity of communication system simulation programming [11].

When a single transmit antenna is selected, the highest shadowing coefficient between the transmitting and receiving antenna constellation has been presented at transmit antenna selection (TAS) [12]. The error probability, which is caused by fading and shadowing problems for multiple wireless systems, is presented [13]. It is investigated under different users' signal power ranges to study the efficient transmission of multi-user channels with universal mobile telecommunication system (UMTS), global system for mobile communications (GSM), wireless local area network (WLAN) systems, and Bluetooth at these power values. Accuracy and low computational complexity can be provided using a PDF algorithm to calculate the error probability over Rayleigh fading-shadowing effects of the multiple wireless systems. The proposed model has been operated using different users' signal power as [0.1, 0.2, 0.3] PW of WLAN and Bluetooth, [1, 2, 3] PW of UMTS and GSM systems, [10, 20, 30] PW of power line carrier (PLC), and power liens communication for AC electric power transmission. The simulation program results show that the compensation of the Rayleigh fading and shadowing model over signal to noise ratio (SNR) can present low values of error probability. Furthermore, the probability of error decreases when the SNR increases. Also, the probability of error has been enhanced as the power of the transmitted signal decreases.

The error probability caused by the effect of reflected, refracted, scattering, multipath propagation of signals, shadowing, and fading has been enhanced based on zero-forcing (ZF) adaptive equalizer [14]. The ZF adaptive equalizer with quadrature phase shift keying (QPSK) and 8-PSK modulation can improve the performance of the two-hop link for the Rayleigh and Nakagami-m fading channels [15]. A frequency selective fading channel can evaluate the ZF linear equalizer performance for the single carrier massive multi-input multi-output (MIMO) uplink systems. The linear zero-forcing (LZF) equalizer has been operated for different system parameters, such as the signal-to-interference plus noise ratio (SINR) and the antenna numbers, to provide their impacts on the system performance PDF has been used for the outage error probability derive [16]. The ZF algorithm as a linear detection method has been presented in 5G massive multiple users' systems. It is low complexity compared with other detection algorithms. The matrix inversion operation, with few simple iterations, is avoided, and full use of soft information is obtained. The ZF is one of the most efficient solutions for the signal detection of massive MIMO systems. Also, the linear equalizer is designed to produce an ISI and provide frequency diversity to noise enhancement [17]. The diversity of symbol-by-symbol ZF equalizers is one regardless of channel memory length. This paper presents a low-complexity analysis of BER enhancement for 5G MIMO communication wireless systems based on an LZF equalizer. It investigates the error probability regarded the fading-shadowing, noise, and ISI effects of low-distance communications systems. Different numbers of 5G antenna constellations are investigated using MATLAB simulation. The relationship between the BER and SNR is investigated.

2. THE PROPOSED MODEL

In this section, we consider the Rayleigh-fading channel, shadowing and path losses, and AWGN noise with a mobile wireless communication system, as shown in Figure 1. Also, ISI is considered in 5G massive MIMO systems. The transmitted signal power has been selected for a specific type of application, such as industrial and real-time applications. The relationship between the BER with different SNR values has been analyzed for a different number of 5G antennas constellation $T_x \times R_x$ such as 8×8 , 8×10 , 8×12 , 8×14 , 8×16 , and 8×18 . A 256 quadrature amplitude modulation (QAM) with the LZF equalizer has been used to reduce the BER caused by fading-shadowing, path losses, noise, and ISI effects of other low-distance communication systems. These effects are presented by a uniform noise channel environment, which is

realized by assuming the equally Rayleigh-fading-shadowing, path losses, AWGN, and ISI effects in all directions and constant time intervals. As shown in Figure 1, there is an LZF-fading shadowing, path losses, AWGN noise, and ISI of MIMO uplink system model, T_x is the transmit antennas constellation, and R_x is the receive antennas constellation, which is presented with the uplink with base station (BS) and down link at mobile station (MS), respectively.

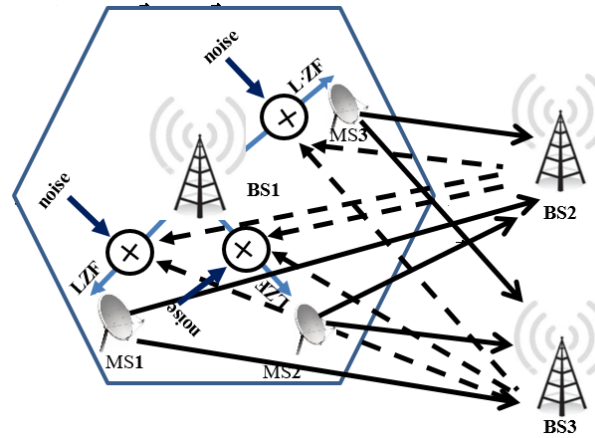


Figure 1. LZF-fading shadowing, path losses, AWGN, and ISI model of MIMO uplink-downlink system

The shadowing effects with Rayleigh-fading channel, path losses, AWGN, and ISI have been studied between the T_x and R_x antennas constellation with variant range values (0-18 dB) SNR. The receiving signal of a k subcarrier multi-user system with U users and a b sub-bands at the MS of the MIMO uplink system model is represented as (1) [1], [6], [16], [18]:

$$Y_{j,u,k,b}^i = \alpha_{u,b}^i [H_{j,u,b}^i]^T x_{k,b}^i (n-1+1) + S_{u,k,b} \quad (1)$$

Where $H_{j,u,b}^i = [\alpha_{u,b}^1 h_{j,u,b}^1 \ \alpha_{u,b}^2 h_{j,u,b}^2 \ \dots \ \alpha_{u,b}^i h_{j,u,b}^i]$ is the total frequency channel with a diagonal matrix between the j th transmit antenna and the receive antenna. $H_{j,u}^i$ is the $T_x \times R_x$ channel matrix of Rayleigh fading coefficients matrix between i th and j th transmitter and receiver antennas constellation, respectively. $x_{k,b}^i$ is the vector of symbols, such as $x_{k,b}^i = [x_{k,b}^1 \ x_{k,b}^2 \ \dots \ x_{k,b}^i]^T$ of synchronized single antenna active users at time interval n . $\alpha_{u,b}^i$ is the maximum distance of the path loss and shadowing effect. The $S_{u,k,b}^j$ is the complex AWGN vector of each j th receiver antenna that independent of T_x [7], [13], [19].

$$h_{j,u,b}^i = F_{j,u,b}^i \sqrt{L_{j,u,b} S H_{j,u,b}} \quad (2)$$

Where $F_{j,u,b}^i$ is the effects of the Rayleigh fading for the j th receive antenna. $S H_{j,u,b}$ is the shadowing and the path loss has been presented by $L_{j,u,b}$ as considered as [20]–[22]. The $L_{j,u,b} = d_u (\frac{dis}{dtr})^{\gamma_{u,b}}$ with the d_u is the characteristics of antennas, dis is the antenna far distance field reference, and dtr presents the distance between the transmitter and receiver antenna constellation. $\gamma_{u,b}$ is the path loss exponent propagation of users and subbands [1], [7], [13].

The $K_{T_x} \times K_{R_x}$ total complex channel gain matrix of uth users can be written as (3) [13], [23]:

$$H_{j,u,b}^i = \begin{bmatrix} F_{0,u,b}^0 \sqrt{L_{0,u,b} S H_{0,u,b}} & F_{1,u,b}^0 \sqrt{L_{1,u,b} S H_{1,u,b}} & \dots & F_{(R_x-1),u,b}^0 \sqrt{L_{(R_x-1),u,b} S H_{(R_x-1),u,b}} \\ F_{0,u,b}^1 \sqrt{L_{0,u,b} S H_{0,u,b}} & F_{1,u,b}^1 \sqrt{L_{1,u,b} S H_{1,u,b}} & \dots & F_{(R_x-1),u,b}^1 \sqrt{L_{(R_x-1),u,b} S H_{(R_x-1),u,b}} \\ \vdots & \vdots & \ddots & \vdots \\ F_{0,u,b}^{(T_x-1)} \sqrt{L_{0,u,b} S H_{0,u,b}} & F_{1,u,b}^{(T_x-1)} \sqrt{L_{1,u,b} S H_{1,u,b}} & \dots & F_{(R_x-1),u,b}^{(T_x-1)} \sqrt{L_{(R_x-1),u,b} S H_{(R_x-1),u,b}} \end{bmatrix} \quad (3)$$

where $F_{u,b}(\mu) = \frac{1}{2\delta_{\mu,u,b}^2} \exp\left(-\frac{\mu}{2\delta_{\mu,u,b}^2}\right)$ is the Rayleigh fading as a function of a standard deviation $\delta_{\mu,u,b}^2$ (dB) at $\mu \geq 0$ [13], [23].

The shadowing and path losses with a standard deviation $\delta_{\rho,u,b}^2$ (dB), at $\rho \geq 0$ can be presented as (4) [14], [24]–[26]:

$$LSH_{u,b}(\rho) = \frac{10}{\rho_{u,b}\sqrt{2\pi\epsilon}} \exp\left(-\frac{(\rho)^2}{2\delta_{\rho,u,b}^2}\right) \quad (4)$$

Where $2\delta_{\ln\rho,u,b}^2 = \epsilon$. In (3) can be expressed as a function of standard deviation μ and ρ with dB values [23]–[26].

$$H(\text{dB}) = 10\log_{10} \begin{bmatrix} \mu_{0,u,b}^0 \sqrt{\rho_{0,u,b}} & \mu_{1,u,b}^0 \sqrt{\rho_{1,u,b}} & \dots & \mu_{(Rx-1),u,b}^0 \sqrt{\rho_{(Rx-1),u,b}} \\ \mu_{0,u,b}^1 \sqrt{\rho_{0,u,b}} & \mu_{1,u,b}^1 \sqrt{\rho_{1,u,b}} & \dots & \mu_{(Rx-1),u,b}^1 \sqrt{\rho_{(Rx-1),u,b}} \\ \vdots & \vdots & \ddots & \vdots \\ \mu_{0,u,b}^{(Tx-1)} \sqrt{\rho_{0,u,b}} & \mu_{1,u,b}^{(Tx-1)} \sqrt{\rho_{1,u,b}} & \dots & \mu_{(Rx-1),u,b}^{(Tx-1)} \sqrt{\rho_{(Rx-1),u,b}} \end{bmatrix} \quad (5)$$

Where $F(\text{dB}) = 10\log_{10}\mu_{u,b}$ and $LSH(\text{dB}) = 10\log_{10}\rho_{u,b}$. Figure 2 shows the LZF scheme for fading, shadowing, noise, and ISI of the MIMO up link proposed system.

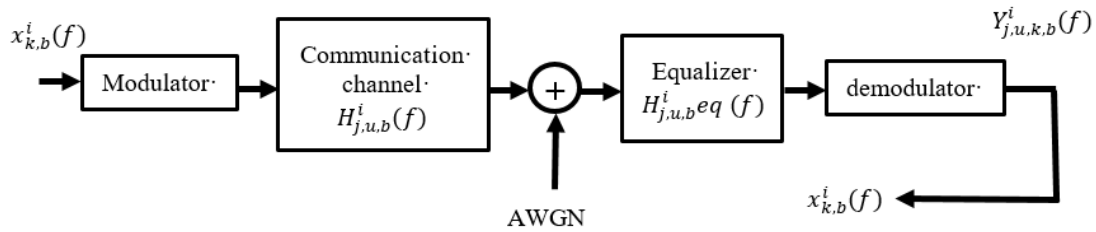


Figure 2. LZF-fading-shadowing, path losses, noise, and ISI system scheme

Assume $H_{j,u,b}^i H_{j,u,b}^{ieq}$ to the corresponding column of Des , which is modelled to detect the desired user symbols vector $x_{k,b}^i(f)(n-L+1)$ [15].

$$x_{k,b}^i(f)(n-L+1) = (des^i)^H(f) Y_{j,u,k,b}^i(f) \quad (6)$$

When $D \leq L$

$$Des = [Des1, \dots, DesL, \dots, DesL+D-1] = H(HH)^{-1} \quad (7)$$

$$des^i = [((des^{i,1})^H, \dots, (des^{i,L})^H, \dots, (des^{i,D})^H)] \quad (8)$$

When $D > L$

$$Des = [Des1, \dots, DesL + [N], \dots, DesL + D - 1] = H(HH)^{-1} \quad (9)$$

$$des^i = \begin{bmatrix} \underbrace{0, \dots, 0}_{noise}, (des^{i,1})^H, \dots, (des^{i,L})^H, \dots, (des^{i,L})^H, \underbrace{0, \dots, 0}_{noise} \end{bmatrix}^H \quad (10)$$

$$x_{k,b}^i(f)(n-L+1) = \underbrace{x_{k,b}^i(f)(n-L+1)}_{desired\ symbol} + \underbrace{\sum_{l=1}^{Lc} (des^{i,l})^H n(n-L+l)}_{Noise} \quad (11)$$

where D is the equalizer length and L is the channel length [15].

The received signal can be written regarded with LZF equalizer as in (12):

$$Y_{j,u,k,b}^i = \sum_{k=-N}^N W_{LZF} x_{k,b}^i \quad (12)$$

The ISI of symbols has been introduced and noise can be enhanced using LZF equalizer. The LZF equalizer can be given by (13) [17]:

$$W_{LZF} = \frac{\|h_{j,u,b}^i F_{j,u,b}^i \sqrt{L_{j,u,b}} S H_{j,u,b}^i\|}{H_{j,u,b}^i H_{j,u,b}^{i eq}} \quad (13)$$

when we assume $\alpha_{u,b}^i [H_{j,u,b}^i]^T$ in (1) equal to C , the LZF equalizer can be written as error estimation in (14) [14], [15], [17], [26]:

$$\begin{aligned} E_{l,n} = & \sum_{L-D+l+1}^L \sum_{j=1}^K \frac{|C_{LD+l+1}(n,j)|^2}{\sum_{L-D+l+1-l+1}^L \sum_{m=1}^M |C(m,j)|^2} \\ & + \sum_l^{L-D+l} \sum_{j=1}^K \frac{|C(n,j)|^2}{\sum_{L-D+l+1-l+1}^{L-D+l+1-l+D} \sum_{m=1}^M |C(m,j)|^2} - \frac{|C(n,j)|^2}{\sum_1^D \sum_{m=1}^M |C(m,j)|^2} \\ & + \sum_1^{l=1} \sum_{j=1}^K \frac{|C(n,j)|^2}{\sum_1^{L-D+l+1-l+D} \sum_{m=1}^M |C(m,j)|^2} \quad 1 \leq l \leq D, \quad 1 \leq n \leq M \end{aligned} \quad (14)$$

The SNR for any CIR realization h and $SNR = \frac{P_o}{N_o}$ is [17], [27].

$$\gamma_{LZF}(SNR, h) \triangleq SNR \left[\frac{1}{2\pi} \int_{-\pi}^{\pi} W_{LZF} du \right]^{-1} \quad (15)$$

The error of ISI caused by composite fading-shadowing and the AWGN noise with all path losses can be calculated by in (16) [23], [26], [28]:

$$\begin{aligned} & \sum_{l=1}^{\min(D,L)} \sqrt{P_u} \alpha_{u,b}^i [H_{j,u,b}^i]^T x_{k,b}^i (n-1+l) \\ & \text{fading - shadowing with path losses} \\ & + \sum_{l=1}^{\min(D,L)} \sum_1^L \sqrt{P_u} \alpha_{u,b}^i [H_{j,u,b}^i]^T x_{k,b}^i (n-L+l-s+1) \\ & \text{ISI} \\ & + \sum_l^{\min(D,L)} \alpha_{u,b}^i n(n-1+l) \\ & \text{noise} \end{aligned} \quad (16)$$

3. SIMULATION RESULTS AND DISCUSSION

The following simulation results present the BER analysis based on SNR related to Rayleigh fading shadowing, path losses, AWGN, and ISI effects channel in multi-user mobile wireless communication systems. The 5G antennas constellation Tx×Rx such as 8×8, 8×10, 8×12, ..., 8×18 with 0-18 SNR range, will be implemented based on the 256 QAM-LZF equalizer. The main parameters of the LZF equalizer model are presented in Table 1. The LZF model simulation model is implemented in MATLAB.

Table 1. The parameters of the LZF equalizer-MIMO system model

LZF model parameters	
Modulation	256 QAM
No. iterations	1,000
No. fast fourier transform (FFT)	128
No. transmitting antennas	8
No. of receiving antennas	8, 10, 12, 14, 16, 18
SNR range	0-18 dB

Figure 3 shows the SNR and BER relationship for a 5G communication MIMO LZF system with 8×8 transmitter and receiver antenna constellation. The BER decreases when SNR increases to reach 0.012875 BER at 18 dB SNR. The BER has been reduced to 0.000625, 3.513×10^{-5} at 16 and 18 dB SNR, respectively, when the receiver antenna number is increased to 10 antennas, as shown in Figure 4. Also, the 8×12 transmitter and receiver antenna constellation are assumed to present the effect of increasing the number of receiver antennas on the 5G LZF equalizer-MIMO system model performance. As a result, the performance of this system has been enhanced, as shown in Figure 5. The BER decreases to 0.000999, 0.000415, 0.00023, and 0.00015 at 12, 14, 16, and 18 dB SNR respectively. Figure 6 shows the relationship between the BER and SNR when the transmitter and receiver are 8×14 antenna constellations. The 5G LZF equalizer-MIMO system model has reached a minimum BER value when the number of receiver antennas increases. The BER reach 0.000859375, 4.232×10^{-5} , 1.510×10^{-5} , 8.031×10^{-6} , and 5.531×10^{-6} at 10, 12, 14, 16, and 18 dB SNR, respectively.

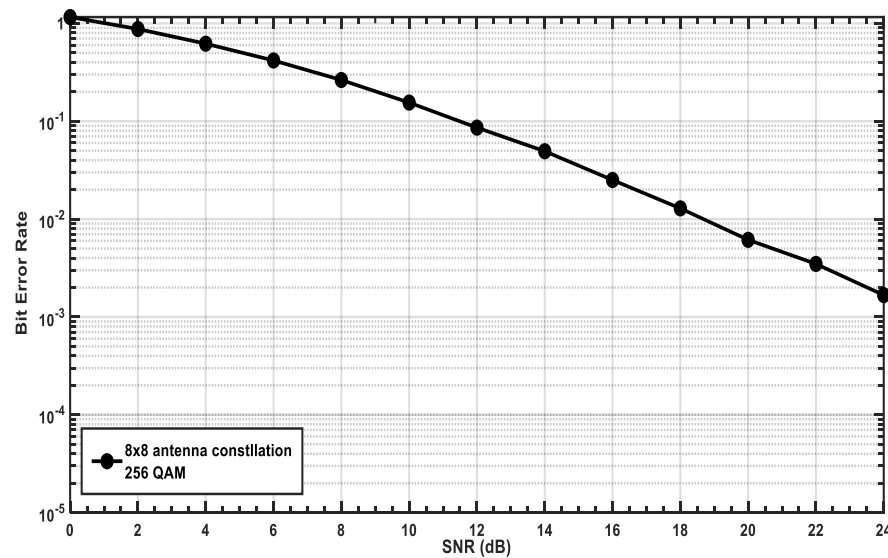


Figure 3. BER of MIMO 8×8 transmitter, receiver antennas constellation, LZF equalizer, and 256 QAM modulation

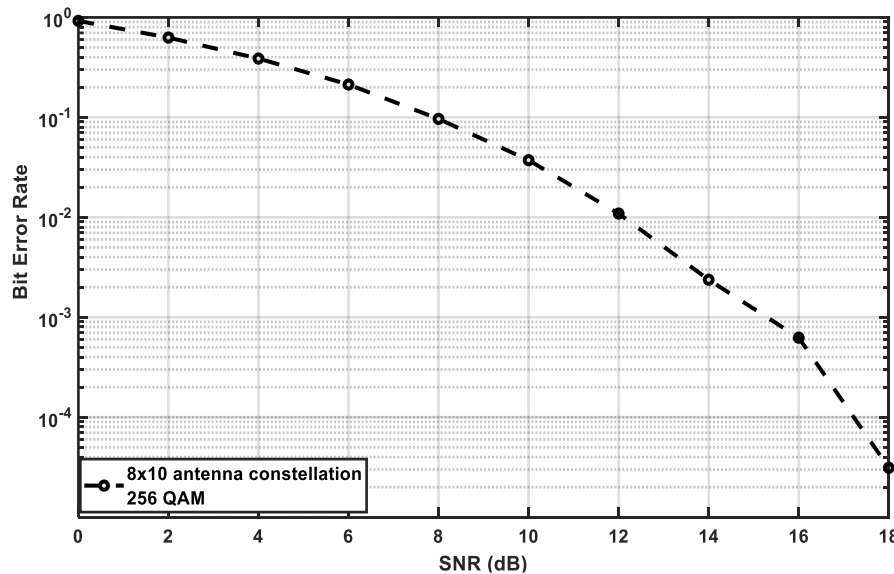


Figure 4. BER of MIMO 8×10 transmitter, receiver antennas constellation, LZF equalizer, and 256 QAM modulation

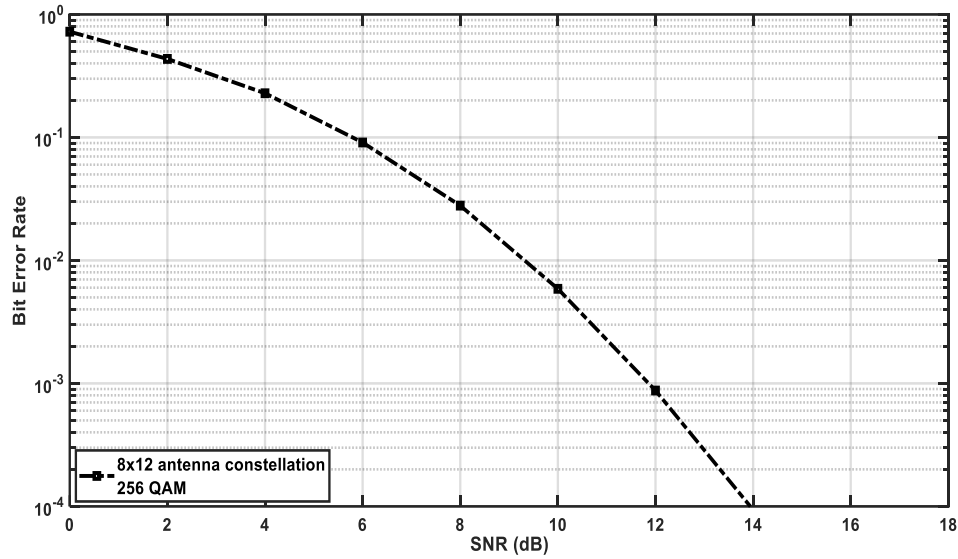


Figure 5. BER of MIMO 8×12 transmitter, receiver antennas constellation, LZF equalizer, and 256 QAM modulation

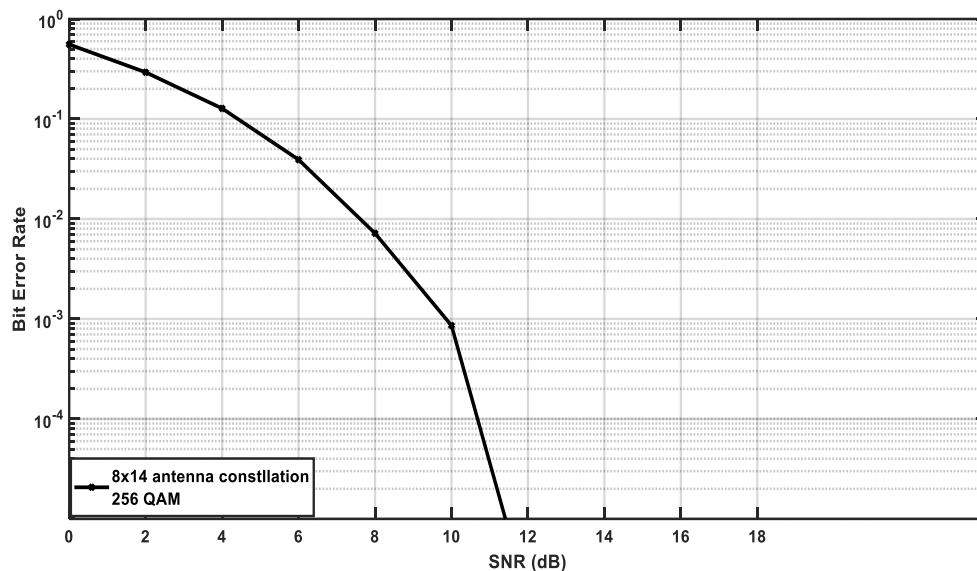


Figure 6. BER of MIMO 8×14 transmitter, receiver antennas constellation, LZF equalizer, and 256 QAM modulation

Figure 7 shows the relationship between the BER and SNR for the 8×16 transmitter and receiver antenna constellation. It can be noted that the BER value reduces until it reaches 0.0001 , 2.033×10^{-5} , 9.04×10^{-6} , 4.22×10^{-6} , and 2.33×10^{-6} at 10, 12, 14, 16, and 18 dB SNR, respectively. The minimum BER value can be obtained from the 8×18 transmitter-receiver antenna constellation, as shown in Figure 8. There are 5.3×10^{-5} , 1.4×10^{-5} , 5.63×10^{-6} , 2.351×10^{-6} , and 1.31×10^{-6} BER at 10, 12, 14, 16, and 18 dB SNR respectively. Table 2 shows the difference between the values of BER when the number of receiver antennas is increased. The BER values can be compared from Table 2 to present the SNR gain obtained when the receiver antenna's number is increased. For 8×10, 8×12, 8×14, 8×16, and 8×18 antennas constellation, the BER values have been compared.

As shown in this table, the high performance of the 5G LZF equalizer-MIMO system model has been provided. Minimum BER values can be caused using the LZF equalizer and then the BER can be reduced based on increasing the receiver antenna constellation. The high performance of these models is

0.000625 and 3.513×10^{-5} of 8×10 can be obtained at 16 and 18 dB SNR, respectively. The BER enhancement can be presented at 16 and 18 dB SNR as 0.000625 and 3.513×10^{-5} , respectively, for 8×12 antenna constellation. The BER enhancement is started at 12 dB SNR. 0.000999, 0.000415, 0.00023, and 1.5×10^{-5} BER can be presented at 12, 14, 16, and 18 dB SNR. For the 8×14 antenna constellation, the high performance of this model can be started from 10, 12, 14, 16, and 18 dB SNR with BER values as 0.0008593, 4.232×10^{-5} , 1.510×10^{-5} , 8.031×10^{-6} , and 5.531×10^{-6} . The same values of SNR as 10, 12, 14, 16, and 18 dB SNR can utilize the minimum value of BER at 8×16 antenna constellation. As shown from BER values, the more efficient LZF equalizer-MIMO system model can be presented at 8×18 as 0.000376, 0.000053, 1.4×10^{-5} , 5.63×10^{-6} , 2.351×10^{-6} , and 1.31×10^{-6} at 8, 10, 12, 14, 16, and 18 dB SNR.

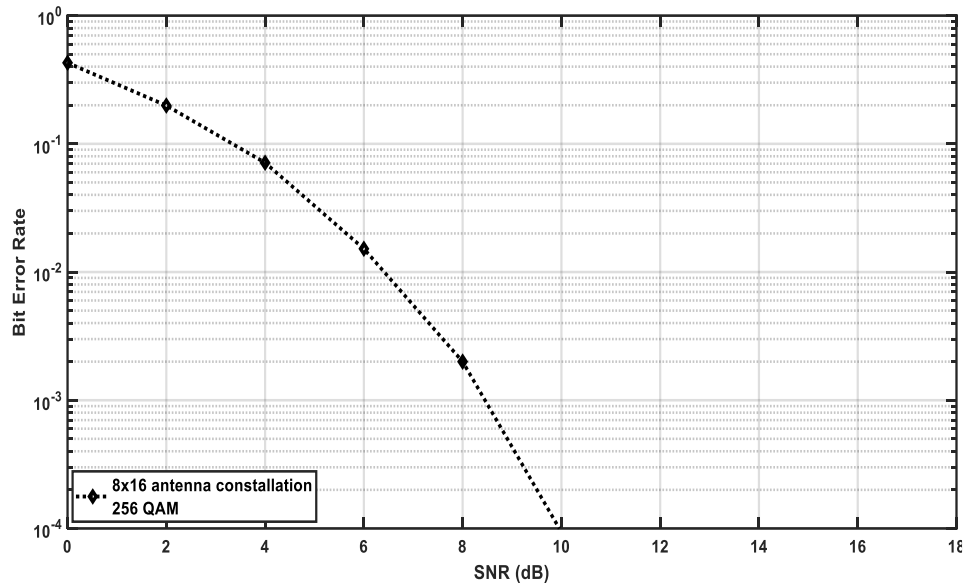


Figure 7. BER of MIMO 8×16 transmitter, receiver antennas constellation, LZF equalizer, and 256 QAM modulation

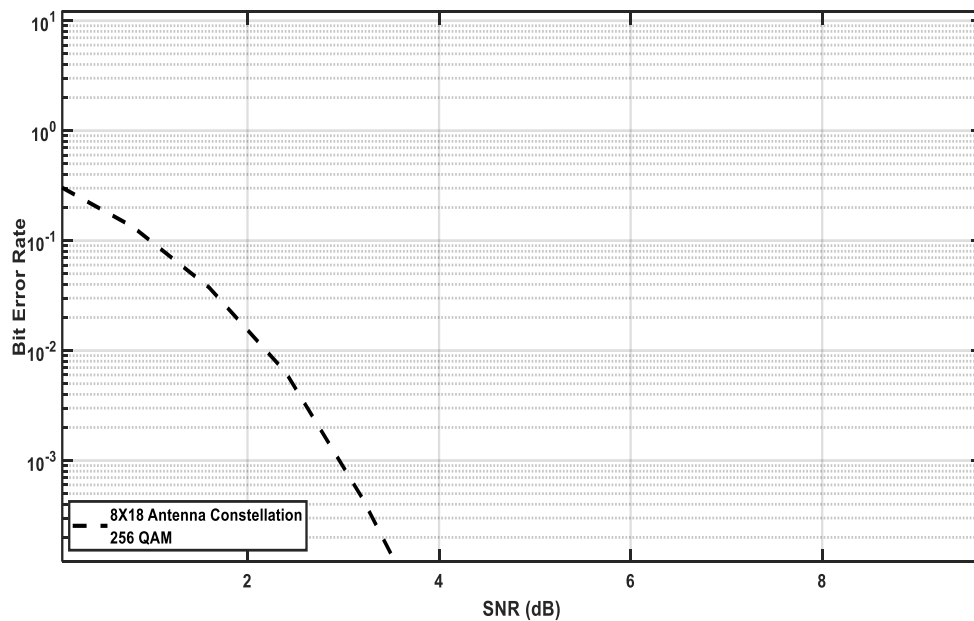


Figure 8. BER of MIMO 8×18 transmitter, receiver antennas constellation, LZF equalizer, and 256 QAM modulation

Table 2. BER of LZF equalizer-MIMO system model for different number of antenna constellation with reference

SNR (dB)	BER of LZF-256 QAM models Transmitting antenna×receiving antenna						Reference conventional algorithm Q-PSK
	8×8	8×10	8×12	8×14	8×16	8×18	
0	1	0.9	0.7	0.556922	0.45	0.305796	0.2
2	0.876433	0.628	0.43475	0.293109	0.198922	0.1265	0.7
4	0.620437	0.387625	0.228578	0.127531	0.0711875	0.036301	0.3
6	0.417859	0.213141	0.0909219	0.0391875	0.0151863	0.005429	0.1
8	0.264062	0.096546	0.0278906	0.0071875	0.002	0.000376	0.02
10	0.155156	0.037281	0.00587	0.0008593	0.0001	0.000053	0.00631
12	0.086109	0.010906	0.000999	4.232×10^{-5}	2.204×10^{-5}	1.4×10^{-5}	0.00201
14	0.049359	0.002375	0.000415	1.510×10^{-5}	9.04×10^{-6}	5.63×10^{-6}	0.001
16	0.025093	0.000625	0.00023	8.031×10^{-6}	4.22×10^{-6}	2.351×10^{-6}	0.00068
18	0.012875	3.513×10^{-5}	1.5×10^{-5}	5.531×10^{-6}	2.33×10^{-6}	1.31×10^{-6}	0.0004066

Figure 9 shows the performance enhancement comparison of different numbers of transmitter-receiver antennas constellation. The 5G LZF equalizer MIMO mobile wireless communication system model reaches high performance when the receiver antenna's constellation is large. As shown in this figure, the low BER values at 8×10, 8×12, 8×14, 8×16, and 8×18 antennas constellation has been reached to 3.513×10^{-5} , 1.5×10^{-5} , 5.531×10^{-6} , 2.33×10^{-6} , and 1.31×10^{-6} respectively at 18 SNR dB.

There is another wireless communication equalization system method, such as the iterative block decision feedback equalizer (IB-DFE). The IB-DFE equalizer can be used with massive MIMO systems. A comparison between the LZE equalizer and IB-DFE [27] has been illustrated in Figure 10. The relationship of BER and SNR for 8×16 and 8×18 antennas constellations is presented to clarify the LZF equalizer efficiency in a massive wireless communication MIMO system. As shown in this figure, the 1.23×10^{-5} and 7.63×10^{-6} BER values have been obtained at 18 dB SNR from 8×16 and 8×18 antennas constellation.

Furthermore, the lower BER values have occurred at 18 dB SNR as 2.33×10^{-6} and 1.31×10^{-6} , when the LZF equalizer is operated. Therefore, at 10^{-5} BER, there is a 4 dB gain of SNR at 8×18 antenna constellation for LZF equalizer than IB-DFE. Also, at 10^{-5} , there is a 4 dB gain of SNR at 8×16 antenna constellation for LZF equalizer than IB-DFE.

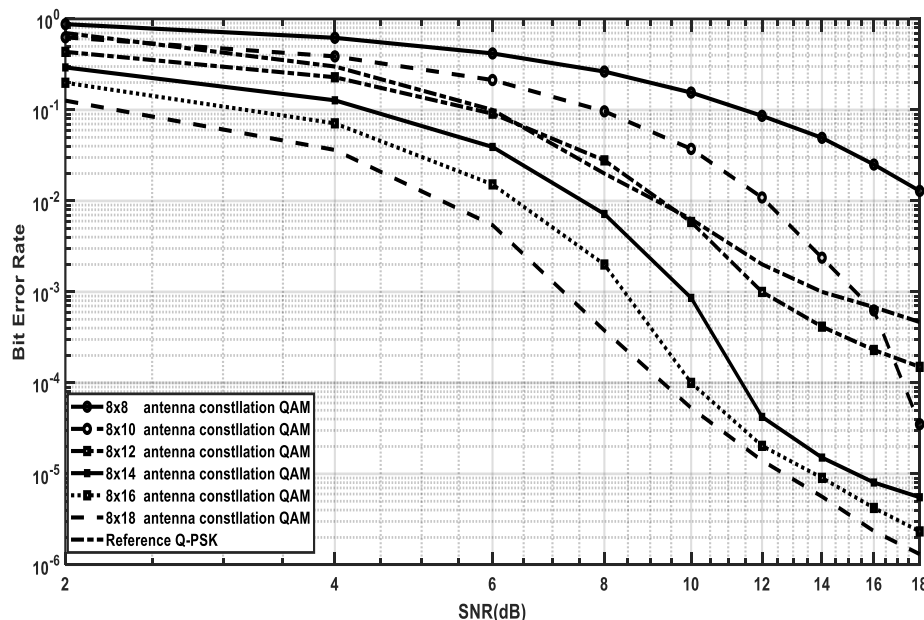


Figure 9. Comparison for different numbers of receiver antenna constellation of LZF equalizer-MIMO QAM system model with error detection Q-PSK reference

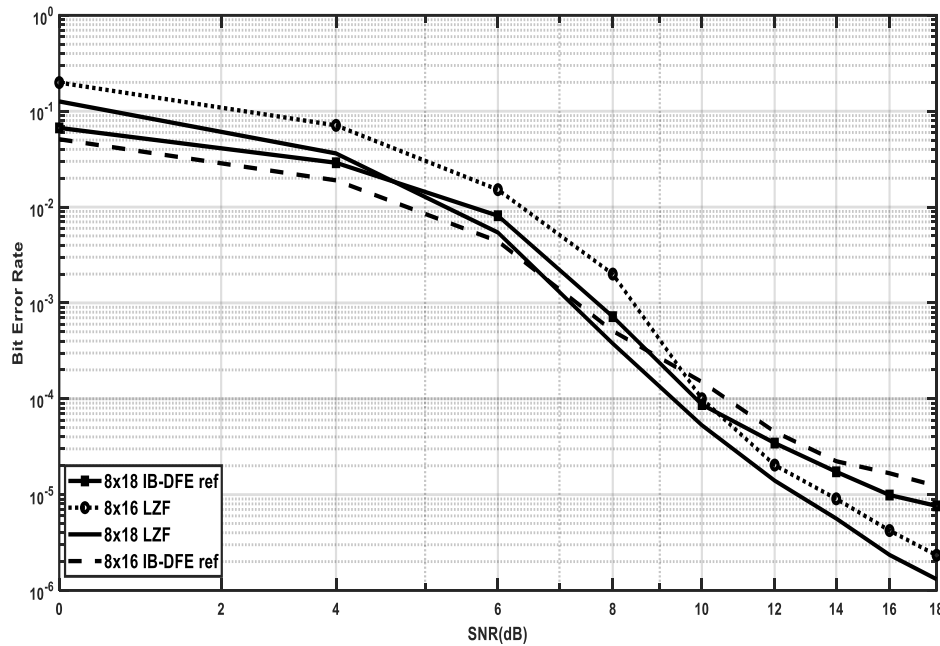


Figure 10. Comparison of LZF equalizer-MIMO with IB-DFE-MIMO systems models with 8×16 and 8×18 antennas constellation

Table 2 shows the BER values of different antennas constellation. The 5G LZF equalizer-MIMO system model has reduced the BER of multi-carrier systems. The high performance of this model is obtained at large numbers of receiver antennas of MIMO systems. Compression between the 5G LZF equalizer-MIMO system model and conventional algorithm QPSK model can be presented to show the enhancement of the suggested model on the BER values.

The SNR gain for a different number of antenna constellations has been summarized as shown in Table 3. The average SNR gain of the LZF equalizer-MIMO system is 1-2 dB range. Therefore, the lower BER values can be satisfied with this model at 8×14 , 8×16 , and 8×18 antennas constellation.

Table 3. SNR gain of LZF equalizer-MIMO system model for different number of antenna constellation

No. of receiver antennas	BER	Gain (dB)
8 to 10	10^{-2}	≈ 6
10 to 12	10^{-2}	≈ 3
	10^{-3}	3
12 to 14	10^{-2}	≈ 2
	10^{-3}	2
14 to 16	10^{-2}	2
	10^{-3}	1.5
	10^{-4}	1.5
	10^{-5}	1
	10^{-6}	≈ 2
16 to 18	10^{-2}	1
	10^{-3}	≈ 1.5
	10^{-4}	0.5
	10^{-5}	1.5
	10^{-6}	2

4. CONCLUSION

The 5G LZF equalizer-MIMO system model is suggested at 0.3 W transmitted power and 265 QAM. Accuracy, low computational complexity and high efficiency can be provided using the LZF equalizer algorithm to calculate the BER of this system with the ISI error caused by composite fading-shadowing, the AWGN noise, and all path losses of the multiple wireless systems. The proposed model has been operated using different numbers of receivers such as 8×10 , 8×12 , 8×14 , 8×16 , and 8×18 antennas constellation. The simulation results show that the compensation of Rayleigh fading shadowing, path losses, and AWGN noise model can provide a low BER value with LZF equalizer-MIMO system.

Moreover, the BER values decrease when SNR increases. Also, the BER can be improved when the number of receiver antennas is increased. Finally, lower BER will be included for 5G multi-user mobile wireless communication systems when the LZF equalizer is operated at large numbers of receiver antennas.




REFERENCES

- [1] H.-M. Chen, C. Zhang, and M. Chen, "Outage Probability Analysis of the Downlink ST-MRC Distributed Antenna System over Shadowed Rayleigh Fading Channels," in *2009 5th International Conference on Wireless Communications, Networking and Mobile Computing*, pp. 1-4, Sep. 2009, doi: 10.1109/wicom.2009.5301051.
- [2] M. C. Ilter and I. Altunbas, "Physical layer network coding in generalized shadowed fading channels," in *2012 International Symposium on Wireless Communication Systems (ISWCS)*, pp. 746-750, Aug. 2012, doi: 10.1109/iswcs.2012.6328467.
- [3] M. C. Uko, M. A. Umoren, and J. Enyenihi, "Effect of shadowing and multipath fading on the area spectral for cell-edge users in heterogeneous networks," *Nigerian Journal of Technology*, vol. 35, no. 2, pp. 409-414, May 2016, doi: 10.4314/njt.v35i2.24.
- [4] A. Sehgal, R. Agrawal, R. Bhardwaj, and K. K. Singh, "Reliability Analysis of Wireless Link for IOT Applications Under Shadow-Fading Conditions," *Procedia Computer Science*, vol. 167, pp. 1515-1523, 2020, doi: 10.1016/j.procs.2020.03.362.
- [5] T. Shaik and R. Dhuli, "Outage performance of NOMA with interference over κ - μ shadowed faded channels," *AEU-International Journal of Electronics and Communications*, vol. 134, p. 153702, May 2021, doi: 10.1016/j.aeue.2021.153702.
- [6] S.-R. Lee, S.-H. Moon, J.-S. Kim, and I. Lee, "Capacity Analysis of Distributed Antenna Systems in a Composite Fading Channel," *IEEE Transactions on Wireless Communications*, vol. 11, no. 3, pp. 1076-1086, Mar. 2012, doi: 10.1109/twc.2011.122211.110645.
- [7] S. Alam and A. Annamalai, "Energy detector's performance analysis over the wireless channels with composite multipath fading and shadowing effects using the AUC approach," in *2012 IEEE Consumer Communications and Networking Conference (CCNC)*, pp. 771-775, Jan. 2012, doi: 10.1109/ccnc.2012.6181162.
- [8] A. M. Hamed and R. K. Rao, "Energy and spectral efficiencies of M-CPFSK in fading and shadowing wireless channels," *Physical Communication*, vol. 30, pp. 204-212, Oct. 2018, doi: 10.1016/j.phycom.2018.07.013.
- [9] F. Yilmaz and M.-S. Alouini, "Partial relay selection based on shadowing side information over generalized composite fading channels," in *2011 8th International Symposium on Wireless Communication Systems*, pp. 367-371, Nov. 2011, doi: 10.1109/iswcs.2011.6125385.
- [10] A. Dziri, D. L. Ruyet, D. Roviras, and M. Terre, "Outage probability analysis of the decode and forward relaying over the composite fading multipath/shadowing channels," in *2010 IEEE 11th International Workshop on Signal Processing Advances in Wireless Communications (SPAWC)*, pp. 1-5, Jun. 2010, doi: 10.1109/spawc.2010.5670907.
- [11] C. Zhang, X. Chen, H. Yin, and G. Wei, "Two-dimensional shadow fading modeling on system level," in *2012 IEEE 23rd International Symposium on Personal, Indoor and Mobile Radio Communications-(PIMRC)*, pp. 1671-1676, Sep. 2012, doi: 10.1109/pimrc.2012.6362617.
- [12] A. Yilmaz, F. Yilmaz, M.-S. Alouini, and O. Kucur, "On the Performance of Transmit Antenna Selection Based on Shadowing Side Information," *IEEE Transactions on Vehicular Technology*, vol. 62, no. 1, pp. 454-460, Jan. 2013, doi: 10.1109/tvt.2012.2220163.
- [13] A. Q. Hameed, "Rayleigh fading-shadowing of outdoor channels analysis based on SNR-PDF model," *Kufa Journal of Engineering*, vol. 10, no. 2, pp. 114-125, Jun. 2021, doi: 10.30572/2018/kje/100209.
- [14] A. S. M. M. Rahaman, M. I. Islam, and M. R. Amin, "Application of Zero-Forcing Adaptive Equalization in Compensation of Fading Effect of Two-hop Wireless Link," *International Journal of Engineering and Technology*, vol. 3, no. 6, pp. 628-631, 2011, doi: 10.7763/ijet.2011.v3.296.
- [15] T. Li and M. Torlak, "Performance of ZF Linear Equalizers for Single Carrier Massive MIMO Uplink Systems," *IEEE Access*, vol. 6, pp. 32156-32172, 2018, doi: 10.1109/access.2018.2841032.
- [16] I. Khan, M. Zafar, M. Ashraf, and S. Kim, "Computationally Efficient Channel Estimation in 5G Massive Multiple-Input Multiple-output Systems," *Electronics*, vol. 7, no. 12, pp. 1-12, Dec. 2018, doi: 10.3390/electronics7120382.
- [17] A. Tajer, A. Nosratinia, and N. A. -Dhahir, "Diversity Analysis of Symbol-by-Symbol Linear Equalizers," *IEEE Transactions on Communications*, vol. 59, no. 9, pp. 2343-2348, Sep. 2011, doi: 10.1109/tcomm.2011.062311.100285.
- [18] M. Hadzialic, V. Lipovac, and B. Nemsic, "Statistical model for the transitional error probability of shadowing mobile channel," in *MELECON 2008-The 14th IEEE Mediterranean Electrotechnical Conference*, pp. 880-884, May 2008, doi: 10.1109/melcon.2008.4618548.
- [19] L. Bariah, S. Muhaidat, and A. Al-Dweik, "Error Probability Analysis of NOMA-Based Relay Networks With SWIPT," *IEEE Communications Letters*, vol. 23, no. 7, pp. 1223-1226, Jul. 2019, doi: 10.1109/lcomm.2019.2897770.
- [20] Q. He, Y. Hu, and A. Schmeink, "Closed-Form Symbol Error Rate Expressions for Non-Orthogonal Multiple Access Systems," *IEEE Transactions on Vehicular Technology*, vol. 68, no. 7, pp. 6775-6789, Jul. 2019, doi: 10.1109/tvt.2019.2917579.
- [21] I. Trigui, A. Laourine, S. Affes, and A. Stephenne, "Outage Analysis of Wireless Systems over Composite Fading/Shadowing Channels with Co-Channel Interference," in *2009 IEEE Wireless Communications and Networking Conference*, pp. 1-6, Apr. 2009, doi: 10.1109/wcnc.2009.4917874.
- [22] L. Mailaender, "Received Signal Strength (RSS) location estimation with nuisance parameters in correlated shadow fading," in *2012 IEEE International Conference on Communications (ICC)*, pp. 3659-3663, Jun. 2012, doi: 10.1109/icc.2012.6363742.
- [23] A. Palaos, P. Mahonen, and J. Riihijarvi, "Shadow fading correlations with compressive sensing: Prediction accuracy," in *2012 IEEE International Conference on Communications (ICC)*, pp. 4872-4877, Jun. 2012, doi: 10.1109/icc.2012.6364190.
- [24] L. Bariah, S. Muhaidat, and A. -Dweik, "Error Probability Analysis of Non-Orthogonal Multiple Access Over Nakagami-m Fading Channels," *IEEE Transactions on Communications*, vol. 67, no. 2, pp. 1586-1599, Feb. 2019, doi: 10.1109/tcomm.2018.2876867.
- [25] R. Singh and M. Rawat, "On the performance analysis of effective capacity of double shadowed κ - μ fading channels," in *TENCON 2019 - 2019 IEEE Region 10 Conference (TENCON)*, pp. 806-810, Oct. 2019, doi: 10.1109/tencon.2019.8929632.
- [26] Y. Liu, H. Ding, J. Shen, R. Xiao, and H. Yang, "Outage Performance Analysis for SWIPT-Based Cooperative Non-Orthogonal Multiple Access Systems," *IEEE Communications Letters*, vol. 23, no. 9, pp. 1501-1505, Sep. 2019, doi: 10.1109/lcomm.2019.2924655.
- [27] D. Fernandes, F. Cercas, and R. Dinis, "Iterative Receiver Combining IB-DFE with MRC for Massive MIMO Schemes," *Procedia Computer Science*, vol. 109, pp. 305-310, 2017, doi: 10.1016/j.procs.2017.05.356.




- [28] I. Trigui, A. Laourine, S. Affes, and A. Stephenne, "Performance analysis of mobile radio systems over composite fading/shadowing channels with co-located interference," *IEEE Transactions on Wireless Communications*, vol. 8, no. 7, pp. 3448–3453, Jul. 2009, doi: 10.1109/twc.2009.081250.

BIOGRAPHIES OF AUTHORS



Ashwaq Q. Hameed    received a B.Sc. degree in Electrical Engineering from the University of Technology (UOT), Baghdad, Iraq, in 1997, M.Sc. in Communication Engineering from the University of Technology in 1999, and Ph.D. in Communication Engineering from the University of Technology in 2003. She is currently an Associate Professor at the Department of Electrical Engineering, UOT. Her research interests include mobile wireless communication systems, multi-carrier OFDMA, Q-OSTFBC MIMO systems, speech signal processing, e-learning, and radar systems. She was co-author of three published books 1-ANFIS technique for identification of digitally modulated signals using MATLAB, 2017; 2-laser fundamentals, 2016; 3-small and special electric motors and their control technique, 2016. She can be contacted at email: ashwaq.q.hameed@uotechnology.edu.iq.



Ali H. Numan    received a B.Sc., M.Sc., and Ph.D. in Electrical Engineering from the University of Technology, Iraq, in 1999, 2003, and 2009, respectively. He is an associate professor of Electrical Engineering at the Department of Electromechanical Engineering, University of Technology, Iraq. He is the author of over 50 peer-reviewed publications, 3 patent applications, and six books "hybrid nanofluid in power transformer to performance improvement", LAMBERT, 2017, "control and analysis of doubly fed induction generator in wind turbine" LAMBERT, 2018 "small and special electric motor and their control technique", Dar Djlal, 2016, "engineering drawing", MoE, 2012, "industrial science", MoE, 2011. His research interests include power electronics systems and digital signal processing. He can be contacted at email: ali.h.numan@uotechnology.edu.iq.